Spin-S bilayer Heisenberg models: Mean-field arguments and numerical calculations

Martin P. Gelfand
Department of Physics, Colorado State University, Fort Collins, Colorado 80523

Zheng Weihong, C.J. Hamer and J. Oitmaa
School of Physics, The University of New South Wales, Sydney, NSW 2052, Australia

Spin-S bilayer Heisenberg models (nearest-neighbor square lattice antiferromagnets in each layer, with antiferromagnetic interlayer couplings) are treated using dimer mean-field theory for general S and high-order expansions about the dimer limit for $S = 1,\ 3/2, \ldots, 4$. We suggest that the transition between the dimer phase at weak intraplane coupling and the Néel phase at strong intraplane coupling is continuous for all S, contrary to a recent suggestion based on Schwinger boson mean-field theory. We also present results for $S = 1$ layers based on expansions about the Ising limit: In every respect the $S = 1$ bilayers appear to behave like $S = 1/2$ bilayers, further supporting our picture for the nature of the order-disorder phase transition.

PACS numbers:

I. INTRODUCTION AND MEAN-FIELD ARGUMENTS

The bilayer Heisenberg antiferromagnet,

$$H = J_1 \sum_{a=1,2} \sum_{\langle i,j \rangle} \mathbf{S}_{a,i} \cdot \mathbf{S}_{a,j} + J_2 \sum_i \mathbf{S}_{1,i} \cdot \mathbf{S}_{2,i} \ , \qquad (1)$$

where the intralayer couplings run over nearest neighbors on square lattices and the $\mathbf{S}$ are $S = 1/2$ quantum spins, has turned out to be an excellent testing ground for notions of quantum criticality. A variety of controlled calculations, such as strong-coupling expansions at zero temperature (starting with the work of Hida[1] and extended by two of the present authors[2,3]), finite-temperature quantum Monte Carlo calculations[4,5] and high-temperature expansions[6] fit extremely well into the general field-theoretic framework for zero-temperature order-disorder critical points in unfrustrated two-dimensional quantum antiferromagnets.[7]

The critical point in the $S = 1/2$ bilayer Heisenberg model is between a Néel ordered phase when $\lambda \equiv J_1/J_2$ is sufficiently large (greater than the critical value $\lambda_c = 0.394$) and a magnetically disordered "dimer" phase which is the adiabatic continuation of the $\lambda = 0$ ground state (which is a product of interlayer singlet pair wavefunctions). The universality class of the phase transition is the same as for finite-temperature transitions in $d = 3$, $O(3)$ symmetric models.

It seemed most natural to us that for larger values of the quantum spin S the same scenario would play out: The value of λ_c would change, but qualitatively nothing would be different. It therefore came as a surprise when Ng, Zhang, and Ma[8] described the results of Schwinger boson mean-field (SBMF) calculations, which indicate that for $S > S_c$ the transition between magnetically ordered and disordered phases is *first-order*. The calculation leads to $S_c \approx 0.35$, and hence indicates that for all physical values of S the transition should be first-order; but it is reasonable to accept the suggestion of Ng *et al.* that SBMF theory leads to phase diagram of S versus λ which is qualitatively valid even if S_c is underestimated. Two more salient points regarding the SBMF results should be noted. At large S, the value of λ at the dimer-Néel phase boundary scales as $1/S$; and at sufficiently large S the ground state on the dimer side of the boundary is the pure interlayer singlet pair state (*i.e.,* identical to the ground state at $\lambda = 0$).

Here we will argue that the results of SBMF theory for phase transitions in the bilayer Heisenberg model are qualitatively incorrect, even in the limit of large S where one might expect such an approximation to be reliable.

Ng *et al.* offer an elementary argument in support of their proposed scenario, which it is informative to reconsider. They note that the ideal Néel state and the interlayer singlet state become degenerate for $\lambda = \lambda_1 = O(1/S)$ (with the interlayer singlet state energetically favored for $\lambda < \lambda_1$), while linear spin-wave theory indicates that the magnetization should vanish at $\lambda = \lambda_2 = O(1/S^2)$ (with Néel order existing for $\lambda > \lambda_2$). At large S, it is clear that $\lambda_1 > \lambda_2$. Ng *et al.* suggest that, on decreasing λ from infinity, the transition that one might suspect should take place at λ_2 (presumably a continuous transition from the Néel to dimer phase) is pre-empted by a first-order transition at λ_1. This is certainly consistent with their SBMF calculations.

However, we suggest an alternative interpretation. We believe that the argument in favor of a first-order transition at λ_1 is too simplistic: Using simple trial states to represent the ground states in the respective phases is dangerous, particularly since it is a comparison of subleading (in powers of S) terms in the variational energies for each phase which leads to the estimate for λ_1. Furthermore, there is an elementary calculation which strongly suggests that the dimer phase is unstable with respect to the development of Néel order for $\lambda > \lambda_3 = O(1/S^2)$. Consider a single dimer, subject to a staggered magnetic field which is produced self-consistently by the staggered magnetization of the sys-

tem. Let $J_2\chi_0(S)$ denote the staggered susceptibility of a single dimer. Then, within this "dimer mean-field approximation" one has $\lambda_3 = 1/4\chi_0$. One can calculate χ_0 directly from second-order perturbation theory, based on explicit formulae for 3-j symbols,[9] to find that $\lambda_3 = 3/16S(S+1)$. As promised, the domain of stability of the dimer phase is $O(1/S^2)$, in agreement with the spin-wave estimate for the stability of the Néel phase.

It should be clear that the dimer mean-field approximation underestimates the stability of the dimer phase, just as the standard Weiss theory overestimates Curie temperatures. One could reasonably object to our argument, then, by suggesting that the corrections to this mean-field theory could be large: in particular, λ_3 might be pushed up to a value of order $1/S$. In the following section, we describe high-order perturbation expansions about $\lambda = 0$ for bilayers with $S = 1,\ 3/2, \ldots,\ 4$. Combined with the existing results for $S = 1/2$, they strongly suggest that the corrections to dimer mean-field theory are order unity rather than order S. In addition, for $S = 1$ bilayers we present a wide variety of results based on expansions about $\lambda = 0$ and about Ising models. They are all qualitatively similar to what is found for $S = 1/2$ bilayers, providing additional confirmation that the phase diagram is unchanged with increasing S (in particular, there is no evidence for any phase besides dimer or Néel) and offering accurate results which could prove useful in interpreting data from experimental realizations of $S = 1$ bilayers.

II. SERIES EXPANSIONS AND EXTRAPOLATIONS

A. Triplet Gap and Antiferromagnetic Susceptibility

Perturbation expansions[10] for the ground-state energy E_0, the triplet excitation spectrum, and the antiferromagnetic susceptibility χ have been carried out for bilayers with all integer and half-integer values of S from 1 to 4. The series coefficients for integer S bilayers for the minimum gap Δ, corresponding to wave vector (π, π), and χ are presented in Table I. For $S = 1/2$ bilayers such expansions have already been presented by Zheng[3] to $O(\lambda^{11})$.

Fig. 1 is a set of "scatter plots" of estimated critical λ values versus estimated critical exponents derived from unbiased Dlog-Padé approximants to the gap series for $S = 1$, 2, 3 and 4 bilayers. An analogous plot for $S = 1/2$ is presented in Ref. 2. In every case they have very similar character, with nearly all exponent estimates lying slightly above the anticipated value of 0.71, and with clear correlations between critical point and exponent values. (Scatter plots for the antiferromagnetic susceptibility have very similar character; likewise for the gap and susceptibility of half-integer S bilayers.) As S increases the series actually become better behaved, in that the approximants derived from a fixed number of terms are more tightly clustered (neglecting the outliers) and estimated exponents are closer to the expected value. Biasing the exponent one can obtain more precise estimates of the critical points λ_c, as listed in Table II. The trend is clear: with increasing S, the critical value of λ is approaching a constant multiple of the dimer mean-field value $3/16S(S+1)$. If we plot $1/\lambda_c$ as a function of $R \equiv S(S+1)$ (shown in Fig. 2), we can see that the results can be remarkably well fitted by a straight line

$$1/\lambda_c = c(R - R_c) \tag{2}$$

with an intercept at $1/\lambda_c = 0$ slightly above $R = 0$. The constants c and R_c determined by a linear least squares fit are:

$$c = 3.72(1), \quad R_c = 0.068(2)\ . \tag{3}$$

For general S we have found empirically, based on the ground state energy E_0, the minimum triplet gap Δ, and the antiferromagnetic susceptibility χ series for the eight values of S that have been explicitly calculated, that the coefficients of λ^n can be expressed as polynomials of order n in the variable R. For example, to third order

$$\Delta = 1 - (8/3)R\lambda + [(8/9)R - (32/27)R^2]\lambda^2 + [(56/135)R - (116/135)R^2 - (3824/1215)R^3]\lambda^3\ . \tag{4}$$

Further coefficients are listed in the Appendix. One can then define $r = \lambda R$ and consider the $R \to \infty$, $r \to$ const limit. The resulting series in r corresponds to the terms in the double-series (in R and λ) of the form $R^n\lambda^n$. Its Dlog-Padé approximants are as well behaved as the series for the larger values of S shown above, with unbiased approximants clustering and exponent estimates just above the anticipated value. Biasing the critical point estimates leads to a critical r of 0.2691(7) (this is consistent with the value of c in Eq. (3)), so the ratio of the exact critical point value in the large-S limit to that coming from the dimer mean-field theory is 1.435(4).

We can also try to use the double-expansions in R and λ to analytically continue to unphysically small values of S. An interesting feature of the general-S double-series (both for the Δ and χ) is that all terms of the form $R^0\lambda^{n\geq 1}$ appear to have vanishing coefficients. Consequently, for $S = 0$ there is no phase transition to a Néel-ordered state. Presumably there is a critical spin S_c, less than 1/2, at and below which the dimer state is stable for all values of λ. It has not been possible to obtain a reliable estimate of S_c by constructing Dlog-Padé approximants at fixed values of S: for $S \lesssim 0.35$ the approximants depend strongly on the number of terms used. However, the extrapolation from larger S, summarized in Eqs. (2) and (3), suggests that $S_c = 0.064(2)$.

B. Further results for $S = 1$ bilayers

Although we have presented evidence above that the dimer phase is unstable for λ larger than a critical value of $O(1/S^2)$, we did not firmly establish that the structure of the phase diagram is simply dimer phase–critical point–Néel phase. The fact that the unbiased exponent values are consistent with a Lorentz-invariant, $d = 3$, $O(3)$ universality class is certainly suggestive. For the $S = 1$ bilayers we have done much more. In addition to expansions about $\lambda = 0$ we have constructed expansions about Ising models, generating a set of results analogous to those presented by Zheng[3] for $S = 1/2$ bilayers. Taken together, these leave little room for doubt about the phase diagram.

Because the calculations follow those presented in Ref. 3 so closely we refer the reader to Sec. III of that paper for a description of the calculation (note that the parameter y in that paper corresponds to $1/\lambda$). Expansions were obtained to $O(x^9)$ (with x denoting the ratio of transverse to longitudinal exchange strength) for the sublattice magnetization M, uniform transverse susceptibility $\chi_\perp$, and triplet excitation spectrum. From these we could derive the gap to the optical branch of the spin-wave spectrum at wave vectors $(0, 0)$ ($\Delta_{\rm opt}$, the minimum gap) and $(0, \pi)$ (Δ_X), spin-wave velocity v, and spin-wave stiffness ρ_s. The expansion coefficients will not be presented here but are available from the authors on request. Results of series extrapolations are shown in Figs. 3, 4, and 5. They demonstrate that expansions about the Néel state lead to estimates of the domain of stability of the Néel phase which are completely consistent with the critical point found by expanding about $\lambda = 0$. This is nicely confirmed by Fig. 6, which displays the ground-state energy per site. The values from the dimer expansion match very smoothly on to those from the Ising expansion around the critical point, whereas for a first-order transition there would be a discontinuity in slope at the transition. All of the results presented in this subsection represent the best available theoretical values for experimentally accessible properties of Néel-ordered $S = 1$ bilayers, which should prove useful in the interpretation of experimental data if any such systems are studied. (In real compounds single-ion anisotropy is always present to some degree. The present calculations could readily be extended to include such terms in the Hamiltonian.)

Finally, it is amusing to note that in the dimer phase for $S > 1/2$ bilayers, sufficiently close to $\lambda = 0$, there exist spin-2 elementary excitations. Let us consider $S = 1$ bilayers specifically. Triplet spectra for various values of λ in the dimer phase are shown in Fig. 7 while *quintuplet* spectra are shown in Fig. 8. (These spectra are obtained by direct sums of the terms in the series to the maximum order available.) The latter spectra lose physical significance when the quintuplet excitations can decay into multiple triplet excitations. One might imagine this happens for arbitrarily small values of λ, since at $\lambda = 0$ the quintuplet gap is three times the triplet gap. However, the parity, with respect to interchange of layers in the bilayer system, of the quintuplet excitations is opposite to that of the triplet excitations, and symmetry forbids decay of the quintuplet excitations into an odd number of triplet excitations. Hence stable spin-2 excitations lie between the 2-triplet and 4-triplet continua for sufficiently small λ.

III. DISCUSSION

The order-disorder transition in bilayer Heisenberg antiferromagnets appears to be a problem for which Schwinger boson mean-field theory leads to qualitatively incorrect results even in the limit of large S. We have shown by high order perturbation expansions about the limit of uncoupled interlayer singlets that there is strong evidence for continuous transitions between dimer and Néel phases with critical values of J_1/J_2 scaling as $1/S(S + 1)$. There seems to be no evidence in favor of the scenario described by Ng *et al.*,[8] in which the transition would become first-order for sufficiently large S. Of course this does not imply that the phase diagram for bilayer Heisenberg antiferromagnets is completely universal. If further-neighbor interactions or higher-order exchange interactions (for example, terms in the Hamiltonian of the form $(\mathbf{S}_i \cdot \mathbf{S}_j)^2$) were allowed then a wide variety of new phases could be stabilized. However, for the simplest bilayer models it appears that simple arguments based on the instability of the dimer phase to Néel order (using dimer mean-field theory) and the instability of the Néel phase to a spin-disordered phase (using linear spin-wave theory to determine where the staggered magnetization vanishes), which both suggest a critical point at $J_1/J_2 = O(1/S^2)$, are correct.

ACKNOWLEDGMENTS

This work has been supported by NSF Grant No. DMR 94-57928 (MPG) and the Australian Research Council (ZW, CJH and JO).

APPENDIX:

The double expansions in λ and $R \equiv S(S + 1)$ for the ground-state energy per site E_0/N, triplet minimum energy gap Δ, and antiferromagnetic susceptibility χ for spin-S bilayers are presented in full here.

$$\frac{E_0}{NJ_2} = \frac{-R}{2} - \frac{2\,\lambda^2\,R^2}{3} - \frac{\lambda^3\,R^2}{3}$$

$$+\lambda^4\,R^2\,\left(-\frac{1}{5}+\frac{28\,R}{45}-\frac{38\,R^2}{45}\right)$$
$$+\lambda^5\,R^2\,\left(-\frac{2}{15}+\frac{74\,R}{75}-\frac{151\,R^2}{225}\right)$$
$$+\lambda^6\,R^2\Big(-0.095238095+1.18141968\,R$$
$$-1.93520995\,R^2+3.52146794\,R^3-2.4209868\,R^4\Big)$$
$$+\lambda^7\,R^2\Big(-0.071428571+1.28412698\,R$$
$$-4.19416352\,R^2+5.77329638\,R^3-1.84452422\,R^4\Big)$$
$$+O(\lambda^8) \qquad \text{(A1)}$$

$$\Delta = 1-\frac{8\,\lambda\,R}{3}+\lambda^2\,R\,\left(\frac{8}{9}-\frac{32R}{27}\right)$$
$$+\lambda^3\,R\,\left(\frac{56}{135}-\frac{116\,R}{135}-\frac{3824\,R^2}{1215}\right)$$
$$+\lambda^4\,R\,\left(\frac{20}{81}-\frac{655\,R}{189}+\frac{5120\,R^2}{1701}-\frac{48656\,R^3}{15309}\right)$$
$$+\lambda^5\,R\Big(0.166019988-4.50447076\,R$$
$$+8.81922354\,R^2+5.13123542\,R^3-14.6722347\,R^4\Big)$$
$$+\lambda^6\,R\Big(0.112022751-5.43708747\,R+24.41683462\,R^2$$
$$-23.43145101\,R^3+17.32806918\,R^4-21.97846687\,R^5\Big)$$
$$+\lambda^7\,R\Big(0.091548205-6.26174454\,R+45.07198387\,R^2$$
$$-73.28433315\,R^3+29.56605425\,R^4+59.68596039\,R^5$$
$$-106.4935325\,R^6\Big)+O(\lambda^8) \qquad \text{(A2)}$$

$$\chi = \frac{4R}{3}\Big[1+\frac{16\,\lambda\,R}{3}+\frac{\lambda^2\,R\,(-1+140\,R)}{6}$$
$$+\lambda^3\,R\,\left(-\frac{1}{8}-\frac{143\,R}{36}+\frac{2677\,R^2}{27}\right)$$
$$+\lambda^4\,R\Big(-0.10671296-1.45847442\,R$$
$$-33.2428954\,R^2+403.712863\,R^3\Big)$$
$$+\lambda^5\,R\Big(-0.090168701-0.58931360\,R$$
$$-3.49146301\,R^2-221.1724119\,R^3+1622.218477\,R^4\Big)$$
$$+\lambda^6 R\Big(-0.076292486+0.12455955R+2.92215451R^2$$
$$+8.15178055\,R^3-1231.683801\,R^4+6416.371180\,R^5\Big)$$
$$+O(\lambda^7)\Big] \qquad \text{(A3)}$$

[1] K. Hida, J. Phys. Soc. Japan **61**, 1013 (1992).
[2] M. P. Gelfand, Phys. Rev. B. **53**, 11309 (1996).
[3] W.H. Zheng, cond-mat/9701214.
[4] A. W. Sandvik and D. J. Scalapino, Phys. Rev. Lett. **72**, 2777 (1994).
[5] A. W. Sandvik, A. V. Chubukov, and S. Sachdev, Phys. Rev. B **51**, 16483 (1995).
[6] A. W. Sandvik, R. R. P. Singh, and A. Sokol (unpublished); their results are mentioned in Ref. 5.
[7] A. V. Chubukov, S. Sachdev, and J. Ye, Phys. Rev. B **49**, 11919 (1994).
[8] K.-K. Ng, F. C. Zhang, and M. Ma, Phys. Rev. B **53**, 12196 (1996).
[9] M. Rotenberg, R. Bivins, N. Metropolis, and John K. Wooten, Jr., *the 3-j and 6-j symbols* (Cambridge, Massachusetts: The Technology Press, 1959). See especially pp. 4, 12.
[10] H. X. He, C. J. Hamer, and J. Oitmaa, J. Phys. A **23**, 1775 (1990); M. P. Gelfand, R. R. P. Singh, and D. A. Huse, J. Stat. Phys. **59**, 1093 (1990); M. P. Gelfand, Solid State Commun. **98**, 11 (1996).
[11] T. Matsuda and K. Hida, J. Phys. Soc. Japan **59**, 2223 (1990).
[12] A. J. Millis and H. Monien, Phys. Rev. B **54**, 16172 (1996).

FIG. 1. Plots of critical λ values versus critical exponents for *D*log-Pade approximants to the triplet gap series. All approximants that use all available terms in the series (circles) and all but the last term (squares) are displayed. Note that many of the approximants are difficult to distinguish on these plots, but the "outliers" represent single approximants.

FIG. 2. Plot of the inverse of critical point $(1/\lambda_c)$ versus $S(S+1)$: the crosses with error bars are the estimates biased by the critical index, and the dashed line is a linear fit: $1/\lambda_c = 3.72[S(S+1)-0.068]$. The insert enlarges the region near $S=0$.

FIG. 3. Rescaled energy gaps $\Delta_{\rm opt}$ and $\Delta_{\rm X}$ as a function of $J_2/(J_1+J_2)$. The solid curves at large $J_2/(J_1+J_2)$ are extrapolations based on dimer expansions; the crosses with error bars are the estimates from Ising expansions; the long dashed lines at small $J_2/(J_1+J_2)$ are the results of the linear spin-wave theory;[11] and the open circles connected by a short dashed line are results from the theory of Millis and Monien[12] (with ρ_s, an input to their theory, taken from Fig. 5). The vertical dotted line indicates the critical point.

FIG. 4. The staggered magnetization M and uniform perpendicular susceptibility $\chi_\perp$ for $S=1$ bilayers *versus* $(J_2/J_1)^{1/2}$ as estimated by Ising expansions.

FIG. 5. The spin-wave velocity v and the spin-wave stiffness ρ_s *versus* $(J_2/J_1)^{1/2}$ as estimated by Ising expansions. At the critical ratio $J_2/J_1 = 7.18$, the estimate of v from dimer expansions is also shown.

FIG. 6. The rescaled ground-state energy per site $E_0/(4J_1 + J_2)/N$ as a function of $J_2/(J_1 + J_2)$. The crosses with dashed line connecting them are the results from the expansion about the Ising limit, while the solid line gives the results from the dimer expansion.

FIG. 7. Plot of the spin-triplet excitation spectrum $\Delta(k_x, k_y)$ along high-symmetry cuts through the Brillouin zone for the system with coupling ratios $J_1/J_2 = 0.05$, 0.1, 0.12, 0.1393 (shown in the figure from the top to the bottom at (π, π) respectively). The lines are the estimates by direct sum to the dimer series, and the points (circles with error bar for the case of $J_1/J_2 = 0.1393$ only) are the estimates of the Padé approximants to the dimer series.

FIG. 8. Plot of the quintuplet excitation spectrum $\Delta^q(k_x, k_y)$ along high-symmetry cuts through the Brillouin zone for the system with coupling ratios $J_1/J_2 = 0.05$, 0.1, 0.12, 0.1393. The lines are the estimates by direct sum to the dimer series, and the points (circles with error bar for the case of $J_1/J_2 = 0.1393$ only) are the estimates of the Padé approximants to the dimer series.

TABLE I. Series coefficients c_n for dimer expansions of the minimum triplet gap $\Delta = J_2 \sum_n c_n \lambda^n$ and the antiferromagnet susceptibility $\chi = J_2^{-1} \sum_n c_n \lambda^n$ for $S = 1$, 2, 3, and 4 bilayers.

n	$S = 1$	$S = 2$	$S = 3$	$S = 4$
		Minimum triplet gap		
0	1.0000000000	1.0000000000	1.0000000000	1.0000000000
1	-5.3333333333	$-1.6000000000\times10^{1}$	$-3.2000000000\times10^{1}$	$-5.3333333333\times10^{1}$
2	-2.9629629630	$-3.7333333333\times10^{1}$	$-1.6000000000\times10^{2}$	$-4.5629629630\times10^{2}$
3	$-2.7786008230\times10^{1}$	$-7.0826666667\times10^{2}$	$-5.5573333333\times10^{3}$	$-2.5514008230\times10^{4}$
4	$-4.0140832190\times10^{1}$	$-3.5921481481\times10^{3}$	$-6.1199238095\times10^{4}$	$-4.8582313672\times10^{5}$
5	$-3.3454379922\times10^{2}$	$-1.0569742866\times10^{5}$	$-3.5299272466\times10^{6}$	$-4.6061398131\times10^{7}$
6	$-1.0532000998\times10^{3}$	$-9.1597242219\times10^{5}$	$-6.1760036073\times10^{7}$	$-1.3547279280\times10^{9}$
7	$-9.7019942999\times10^{3}$	$-2.6882225528\times10^{7}$	$-3.6317201466\times10^{9}$	
8	$-3.0018452174\times10^{4}$			
9	$-3.0081157280\times10^{5}$			
		Antiferromagnetic susceptibility		
0	2.6666666667	8.0000000000	1.6000000000×10^{1}	2.6666666667×10^{1}
1	2.8444444444×10^{1}	2.5600000000×10^{2}	1.0240000000×10^{3}	2.8444444444×10^{3}
2	2.4800000000×10^{2}	6.7120000000×10^{3}	5.3728000000×10^{4}	2.4880000000×10^{5}
3	2.0721234568×10^{3}	1.7017800000×10^{5}	2.7320720000×10^{6}	2.1109167901×10^{7}
4	1.6499774192×10^{4}	4.1278260778×10^{6}	1.3301975846×10^{8}	1.7154007839×10^{9}
5	1.2891136900×10^{5}	9.8615644145×10^{7}	6.3850802835×10^{9}	$1.3748488989\times10^{11}$
6	9.9036806734×10^{5}	2.3183667236×10^{9}	$3.0164597503\times10^{11}$	$1.0845538535\times10^{13}$
7	7.5397998426×10^{6}	$5.4074404771\times10^{10}$		
8	5.6895542718×10^{7}			

TABLE II. The critical point λ_c for $S = 1/2$ to $S = 4$ estimated by biasing the critical index (where the case of $S = 1/2$ is already reported in Ref. 3), and its ratio to that predicted by dimer mean-field theory. The results of a linear fit, $1/\lambda_c^{\rm fit} = 3.72[S(S+1) - 0.068]$, are also listed.

S	1/2	1	3/2	2	5/2	3	7/2	4
λ_c	0.3942(8)	0.1393(7)	0.07303(10)	0.0453(1)	0.03098(7)	0.02254(5)	0.01716(5)	0.01349(5)
$\lambda_c^{\rm fit}$	0.3942	0.1391	0.07301	0.04532	0.03096	0.02253	0.01714	0.01349
λ_c/λ_3	1.58	1.49	1.46	1.45	1.44	1.44	1.44	1.44

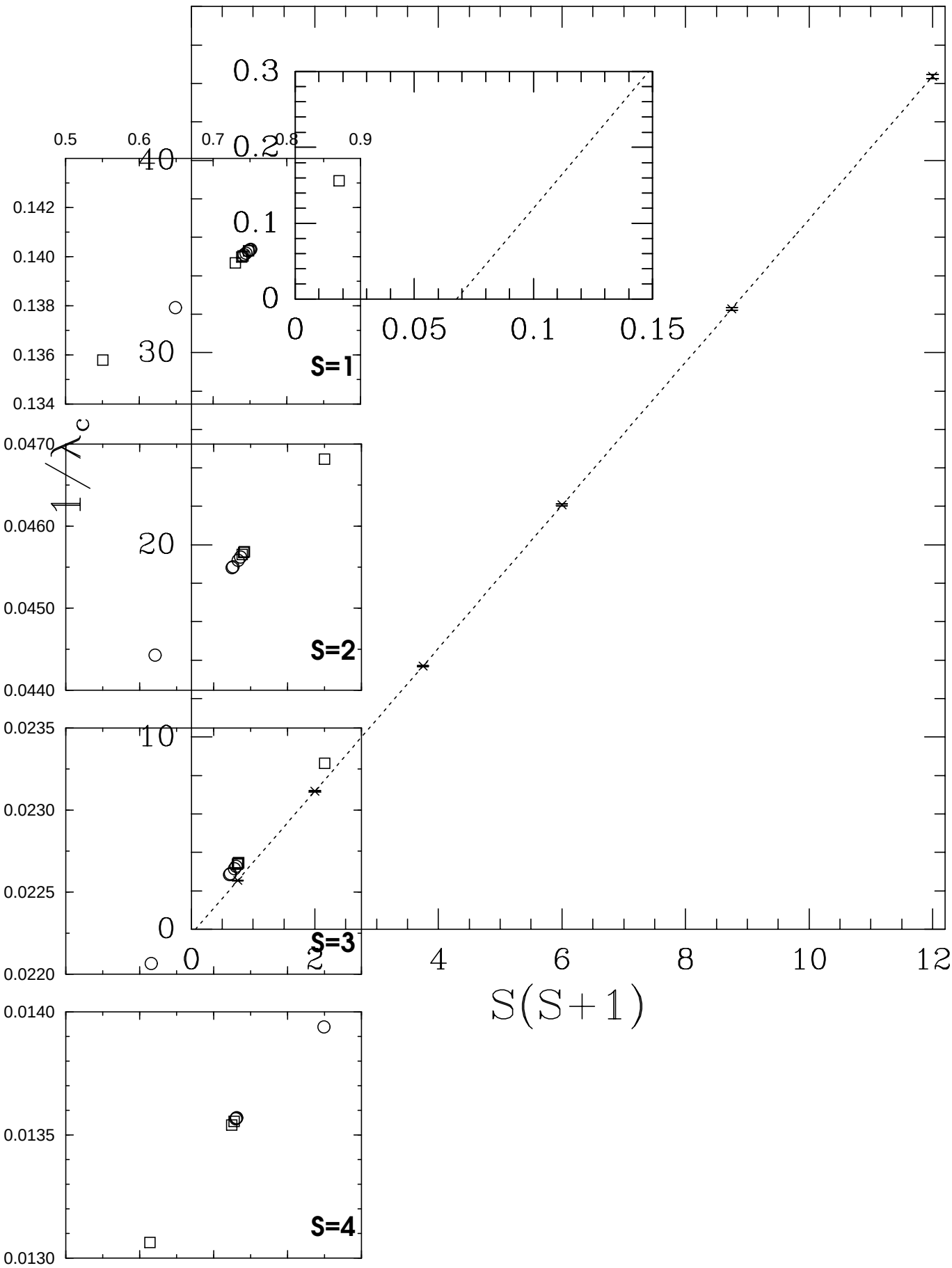
S=1
S=2
S=3
S=4
$1/\chi_c$
S(S+1)

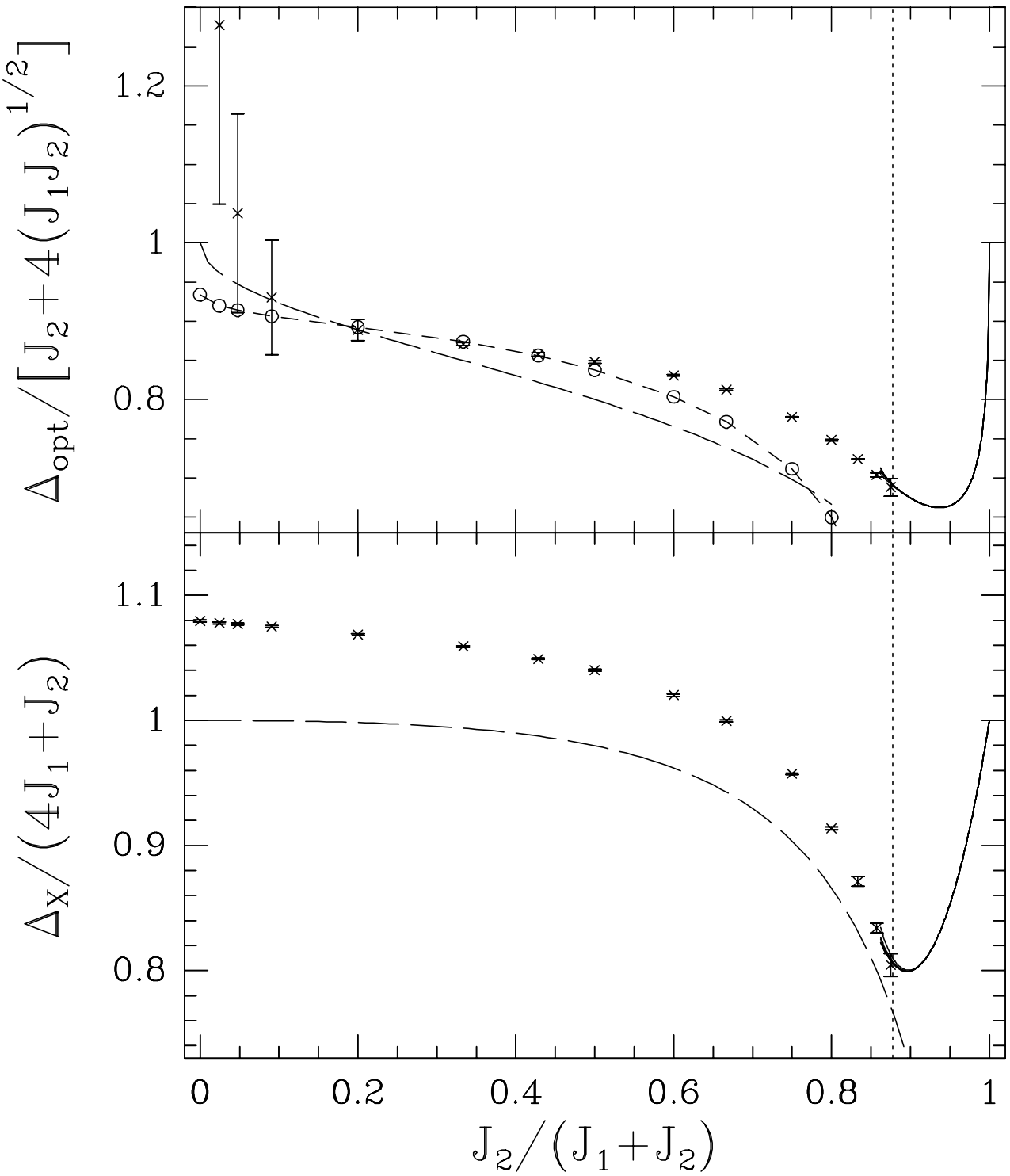
$\Delta_{opt}/\left[J_2+4(J_1J_2)^{1/2}\right]$
1.2
1
0.8
$\Delta_X/(4J_1+J_2)$
1.1
1
0.9
0.8
0
0.2
0.4
0.6
0.8
1
$J_2/(J_1+J_2)$

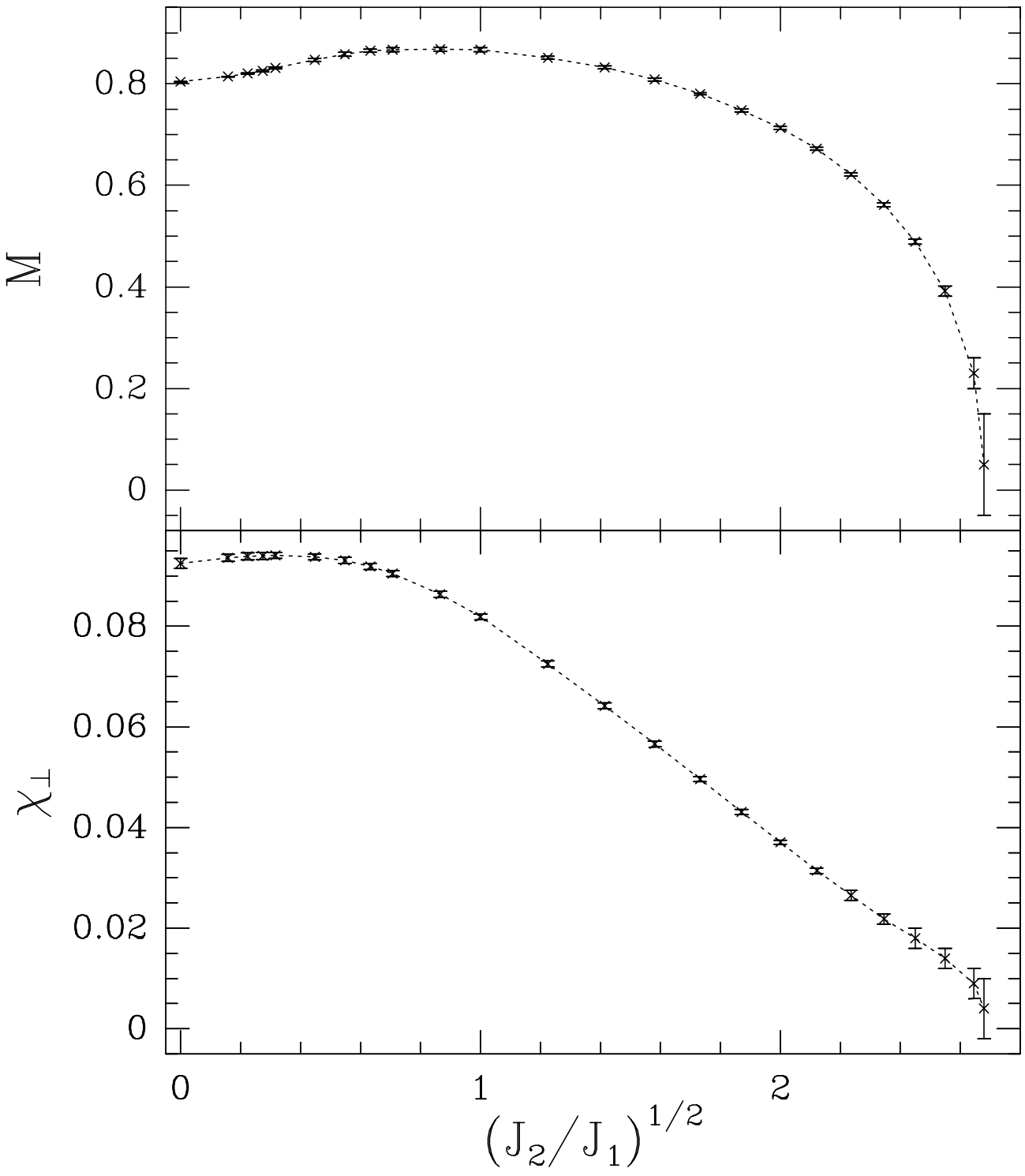
M
0.8
0.6
0.4
0.2
0
$\chi_\perp$
0.08
0.06
0.04
0.02
0
0
1
2
$(J_2/J_1)^{1/2}$

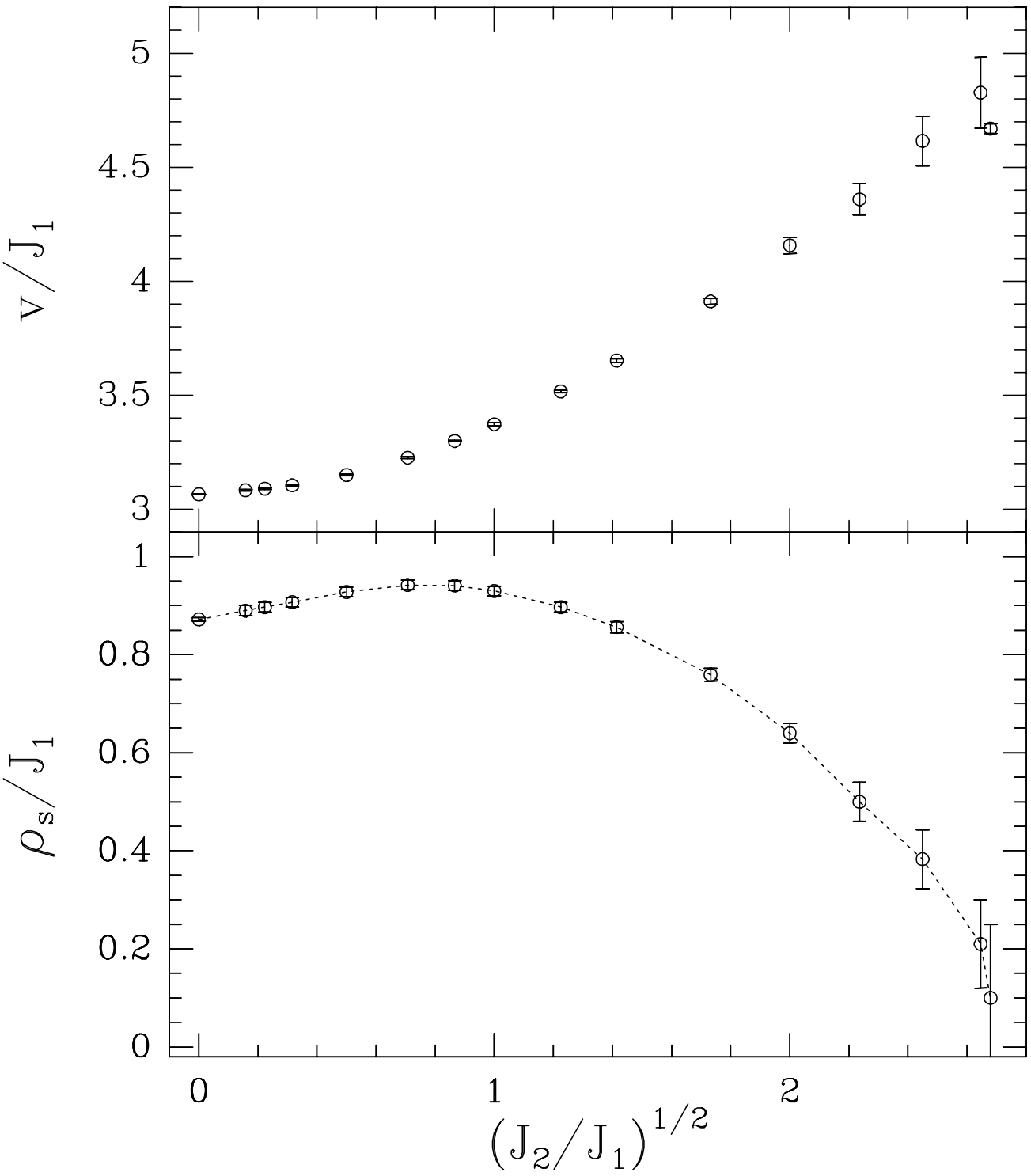
5
4.5
4
3.5
3
V/J1
1
0.8
0.6
0.4
0.2
0
ρs/J1
0
1
2
(J2/J1)1/2

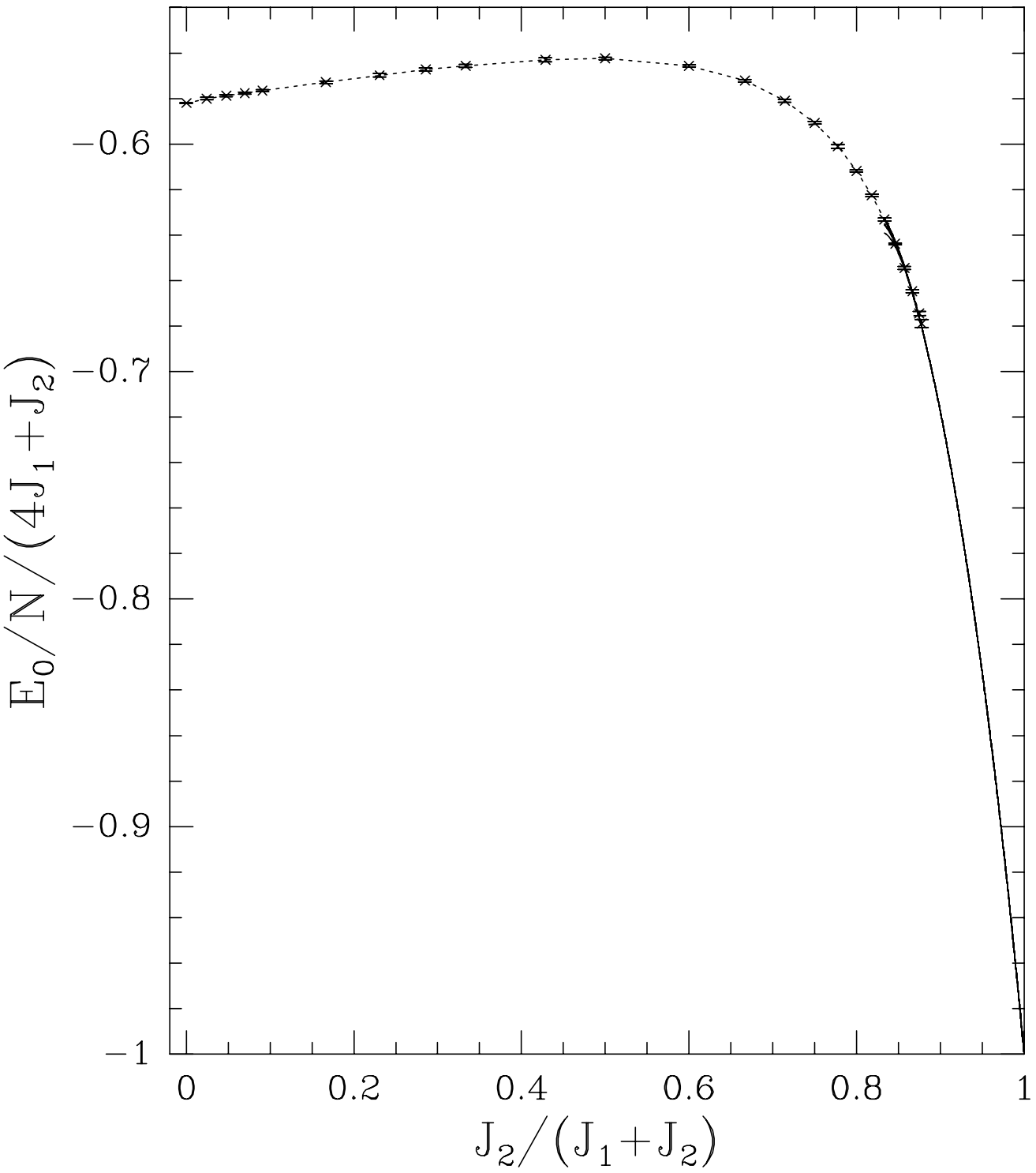
−0.6
−0.7
−0.8
−0.9
−1
0
0.2
0.4
0.6
0.8
1
$E_0/N/(4J_1+J_2)$
$J_2/(J_1+J_2)$

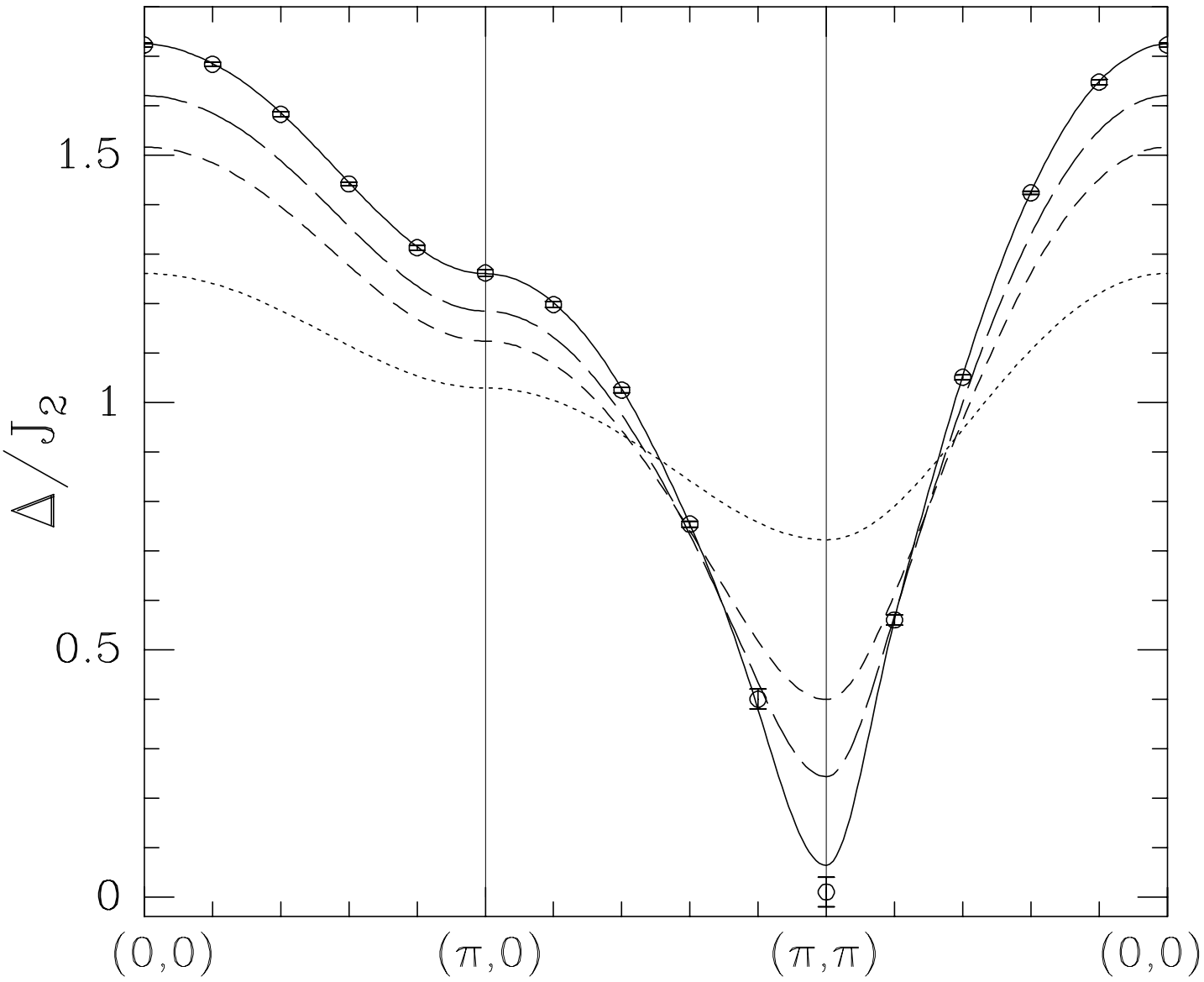
1.5
1
0.5
0
Δ / J_2
(0,0)
$(\pi,0)$
(π,π)
(0,0)

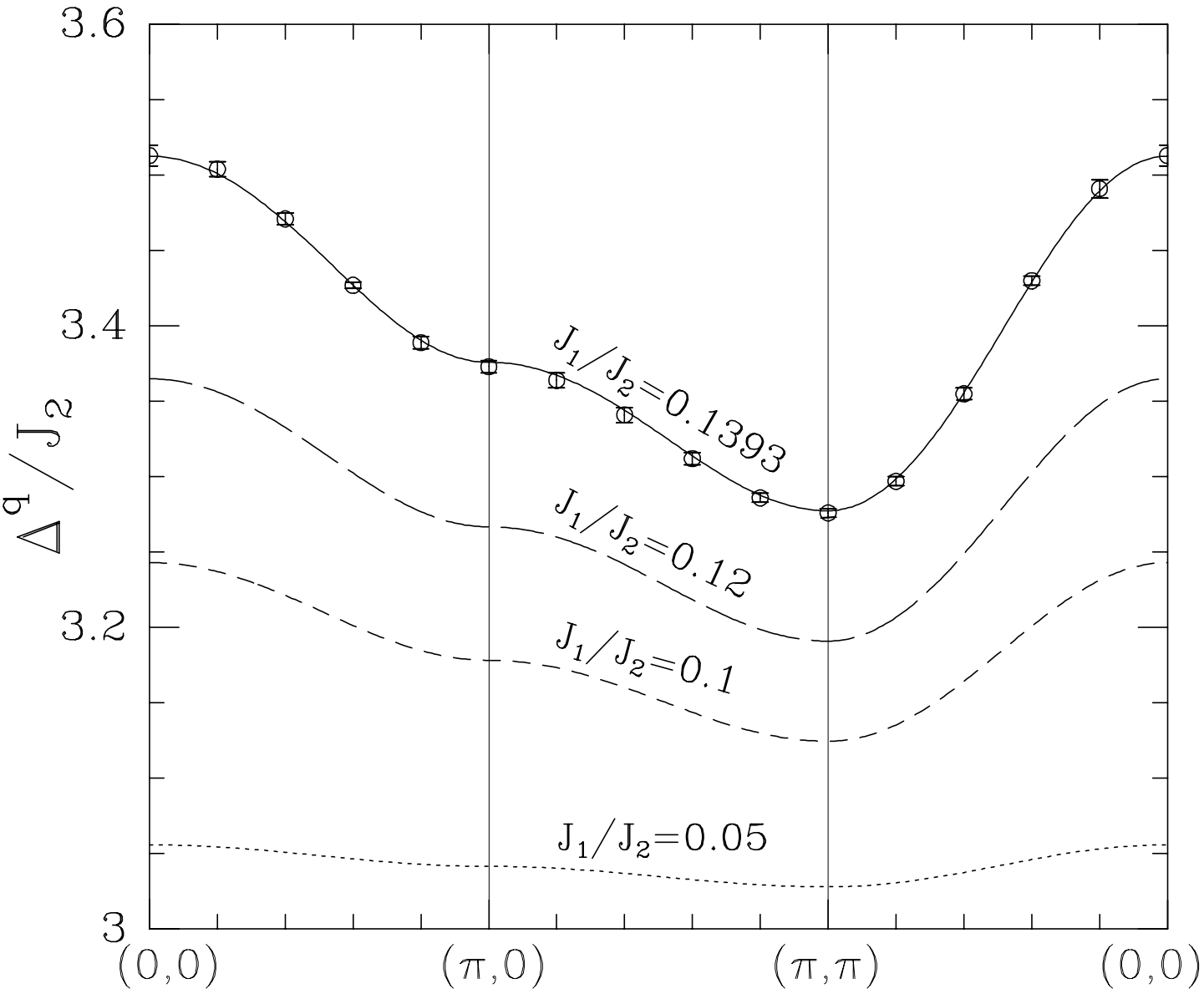
3.6
3.4
3.2
3
Δ^q / J_2
$J_1/J_2=0.1393$
$J_1/J_2=0.12$
$J_1/J_2=0.1$
$J_1/J_2=0.05$
(0,0)
(π,0)
(π,π)
(0,0)